ENHANCED FREQUENCY STABILITY IN AN INVERTER-DOMINATED MICROGRID USING VIRTUAL INERTIA TECHIQUE.

Okpala O.C.[1] Iloh, J.P.I[2] Okonkwo I.I[3]

[1,2,3]*Department of Electrical/Electronic Engineering Chukwuemeka Odumegwu Ojukwu University Uli, Anambra State, Nigeria*
***Corresponding author:** okpalaobinnac@yahoo.com*

ABSTRACT

This study investigates the enhancement of frequency stability in an inverter-dominated photovoltaic (PV) microgrid through the implementation of a Virtual Synchronous Generator (VSG)-based virtual inertia control strategy. The increasing penetration of inverter-based renewable energy sources has led to a significant reduction in system inertia, resulting in faster frequency deviations, higher rates of change of frequency (ROCOF), and reduced stability margins in modern power systems (Fang et al., 2022). These challenges are particularly critical in microgrids operating under weak-grid conditions with limited generation capacity. A model-based simulation approach was adopted to develop and analyse a 2 MW PV-dominated hybrid microgrid located at Nnamdi Azikiwe University, Awka. The system comprises a photovoltaic array, battery energy storage system (BESS), and diesel generator backup. A detailed dynamic model was implemented in MATLAB/Simulink, incorporating a VSG control framework designed to emulate both inertial and damping responses of conventional synchronous generators. The control strategy integrates virtual inertia, damping control, and state-of-charge (SOC)-based energy management within a unified structure. The performance of the proposed system was evaluated under step load disturbances of 2.2 MW, 2.5 MW, 2.8 MW, and 3.0 MW, and compared with a baseline system operating without virtual inertia support. Key performance indicators included frequency deviation, ROCOF, frequency nadir, and settling time. Simulation results demonstrate significant improvements in frequency stability with the implementation of VSG control. Specifically, ROCOF was reduced from −1.25 Hz/s to −0.093 Hz/s at 3.0 MW, while the effective system inertia increased from 0.2 s to approximately 2.7 s. The frequency deviation was also substantially minimised, with the system maintaining operation close to the nominal frequency across all test scenarios. The findings confirm that the proposed VSG-based virtual inertia control strategy effectively enhances the dynamic performance and stability of inverter-dominated microgrids. The relatively low energy requirement for transient support further demonstrates the practical feasibility of the approach. This study contributes to the development of reliable and sustainable microgrid operation, particularly in low-inertia and weak-grid environments typical of developing power systems.

Keywords: Virtual Synchronous Generator (VSG); Frequency Stability; Virtual Inertia; Rate of Change of Frequency (ROCOF); Microgrid Control; Renewable Energy Integration

1.0 INTRODUCTION

The secure operation of electric power systems depends fundamentally on maintaining a continuous balance between power generation and load demand (Okpe *et al*., 2019). When this balance is disturbed, the system frequency deviates from its nominal value, which serves as a primary indicator of system stability. In conventional power systems dominated by synchronous generators, the inherent rotational inertia of generator rotors provides an immediate response to such disturbances. This stored kinetic energy acts as a buffer,

slowing down the rate of frequency change and allowing sufficient time for control mechanisms such as primary frequency regulation to restore equilibrium. As established in classical power system theory, the relationship between power imbalance and frequency dynamics is governed by the swing equation, which highlights the inverse dependence of frequency deviation on system inertia (Kundur, 1994).

The ongoing transition towards low-carbon energy systems has significantly altered this traditional dynamic. The increasing penetration of renewable energy sources, particularly photovoltaic and wind generation, has led to the widespread adoption of power electronic converters for grid interfacing (Odigbo *et al*., 2026). Unlike synchronous generators, inverter-based resources do not possess rotating masses and therefore contribute negligible physical inertia to the grid. As a result, modern power systems are evolving into low-inertia networks characterised by faster frequency deviations, higher rates of change of frequency, and reduced stability margins. This challenge is particularly pronounced in microgrids, which operate with limited generation capacity and are often required to function in islanded modes without support from a strong utility grid (Oyiogu *et al*., 2024).

A growing body of research has examined the implications of reduced inertia on frequency stability and explored potential mitigation strategies. Early analytical studies demonstrated that declining rotational inertia significantly weakens transient stability and increases the severity of frequency excursions following disturbances (Obi *et al*., 2025). These findings have been reinforced by more recent investigations, which show that in inverter-dominated systems, frequency dynamics are no longer governed by electromechanical processes but by converter control strategies. This shift has necessitated the development of artificial inertia mechanisms capable of replicating the stabilising effects of synchronous machines (Fang *et al*., 2022).

Several approaches have been proposed to emulate inertia in inverter-based systems, each with distinct advantages and limitations. One practical method involves integrating battery energy storage systems with photovoltaic generation to provide transient power support. For instance, Wang *et al*. (2014) demonstrated that coordinated control of a battery and PV system could enhance inertial response while maintaining maximum power point tracking. However, although this approach improves short-term frequency stability, it often neglects long-term energy sustainability, particularly with respect to state-of-charge management. In contrast, Rahmann *et al*. (2014) proposed operating photovoltaic systems below their optimal power point to create a reserve margin for frequency support. While effective in principle, this strategy introduces a trade-off between stability and energy efficiency, reducing overall energy yield and limiting applicability under low irradiance conditions.

More advanced control strategies have focused on embedding synchronous generator dynamics directly into inverter control systems. The concept of the synchronverter, introduced by Zhong *et al*. (2012), represents a significant milestone in this direction. By implementing the swing equation within the inverter control architecture, the synchronverter is able to replicate both inertial and damping responses of conventional generators. This framework has since evolved into the widely adopted Virtual Synchronous Generator approach, which offers improved transient performance and enhanced frequency regulation capabilities. Comparative studies indicate that Virtual Synchronous Generator control outperforms traditional droop-based methods, particularly in terms of rate-of-change-of-frequency suppression and frequency nadir improvement (Guerrero *et al*., 2011; Wang *et al*., 2015).

Despite these advancements, ongoing research reveals important limitations in existing virtual inertia techniques. Adaptive control strategies have been proposed to address the variability of operating conditions, with studies demonstrating that dynamically adjusting inertia and damping coefficients can improve system robustness (Sun *et al*., 2020). Similarly, energy-aware control schemes that incorporate battery state-of-charge constraints have been shown to enhance long-term sustainability (Li *et al*., 2021; Zhang *et al*., 2023). However,

these approaches often increase computational complexity and may be difficult to implement in practical microgrid environments with limited control resources. Furthermore, alternative strategies such as Virtual Oscillator Control provide fast dynamic response but lack the intuitive physical interpretation and straightforward tuning associated with swing-equation-based methods (Johnson *et al*., 2013).

Although the theoretical foundation and practical benefits of virtual inertia control are well established, a critical gap remains in the application of these techniques to weak-grid environments, particularly in developing regions. Most existing studies have been validated using laboratory-scale systems, hardware-in-the-loop simulations, or strongly interconnected power networks. In contrast, microgrids in regions such as Sub-Saharan Africa are characterised by low system inertia, high network impedance, limited spinning reserves, and hybrid generation configurations (Chibuzor *et al*., 2025). These factors significantly influence frequency dynamics and may affect the performance of conventional virtual inertia strategies. Consequently, there is limited evidence on the effectiveness of integrated inertia–damping–energy management frameworks in such contexts, especially for photovoltaic-dominated microgrids operating under realistic disturbance conditions.

In light of these challenges, the aim of this study is to enhance frequency stability in an inverter-dominated microgrid through the development and implementation of a Virtual Synchronous Generator-based virtual inertia control strategy. The specific objectives are to develop a detailed dynamic model of a photovoltaic-based microgrid, design a control scheme capable of emulating inertial and damping responses, integrate the proposed control into the system, and evaluate its performance under load disturbance scenarios. Particular emphasis is placed on key performance indicators such as frequency deviation, rate of change of frequency, and frequency nadir.

The primary contribution of this work lies in the coordinated design and validation of a Virtual Synchronous Generator control framework that integrates inertia emulation, damping control, and energy management within a unified structure. Unlike many existing studies, this research applies the proposed methodology to a realistic microgrid model representative of a developing power system environment. The study further provides a comparative analysis of system performance with and without virtual inertia support, thereby offering practical insights into the effectiveness of the proposed approach. Through this, the research contributes to the advancement of reliable and sustainable microgrid operation in low-inertia power systems.

2.0 METHODOLOGY

2.1 Research Design and Approach

This study adopts a model-based simulation approach to investigate frequency stability enhancement in an inverter-dominated photovoltaic (PV) microgrid through the integration of a Virtual Synchronous Generator (VSG) control strategy. The research is structured to enable systematic development, analytical validation, and comparative performance evaluation between a baseline microgrid model (without virtual inertia) and an enhanced system incorporating VSG control.

The methodology is divided into four key stages:

i. data collection and system characterization
ii. mathematical modelling and formulation
iii. control system design and simulation implementation, and
iv. performance evaluation under varying load disturbances.

This structured approach ensures reproducibility and allows for rigorous validation of the proposed control strategy. A time-domain simulation framework was employed to capture transient dynamics such as frequency deviation, rate of change of frequency (ROCOF), and system settling behavior under step load disturbances. The approach enables safe and controlled testing of extreme operating conditions without affecting a real-world system.

2.2 System Model and Framework Description

The system under study is a 2 MW, 11 kV PV-dominated hybrid microgrid located at Nnamdi Azikiwe University (UNIZIK), Awka. The microgrid comprises three major subsystems: the photovoltaic generation unit, battery energy storage system (BESS), and diesel generator backup system.

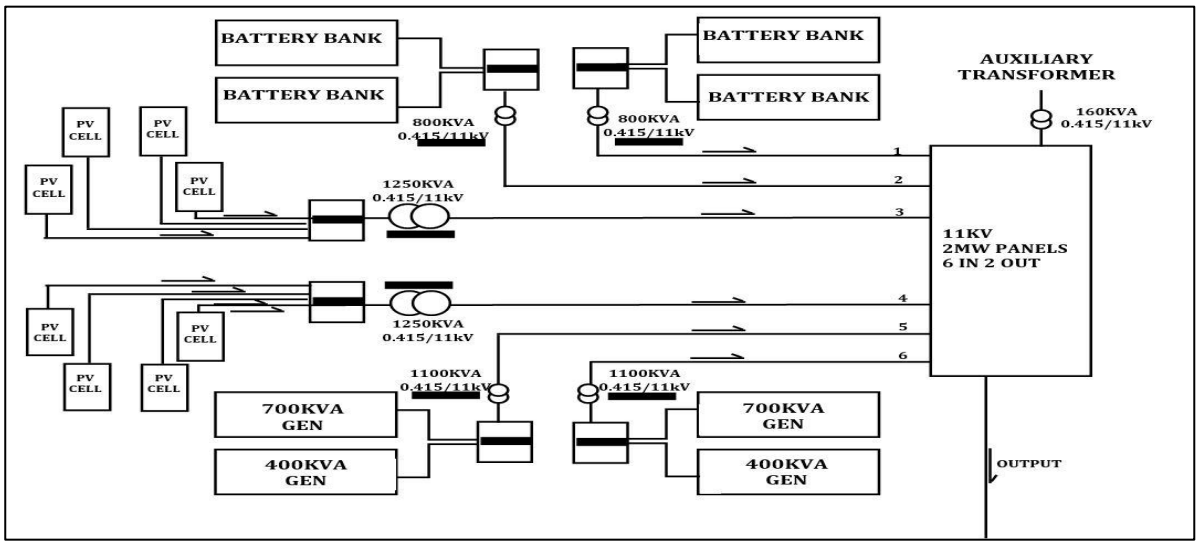

Figure 1: Schematic Block Diagram of the Microgrid Layout at Unizik Awka.

The PV subsystem consists of solar modules rated at 325 W each, arranged in strings of 20 modules connected in series, producing approximately 740 V DC. This output is interfaced through a DC-link to a Voltage Source Inverter (VSI), which converts DC power to 415 V AC. The AC output is subsequently stepped up to 11 kV via a transformer for distribution.

The battery storage system consists of 360 series-connected cells (2 V each), producing a total DC voltage of 720 V. The system supports energy balancing and contributes to frequency stabilization through state-of-charge (SOC)-based control.

The diesel generator subsystem provides auxiliary generation capacity of 1100 kVA, ensuring reliability during low PV generation periods.

The overall system is modeled in a grid-connected configuration, with the Point of Common Coupling (PCC) serving as the interface between the microgrid and the distribution network. The simulation model includes the following components:

i. PV array with MPPT control
ii. DC-link capacitor and voltage regulator

iii. Voltage Source Inverter (VSI)
iv. LC output filter
v. Step-up transformer (415 V/11 kV)
vi. Three-phase distribution network
vii. Variable load blocks

A switching mechanism is implemented to enable comparison between the conventional inverter operation and the VSG-enhanced configuration.

2.3 Mathematical Formulation

The frequency dynamics of the microgrid are derived from the classical swing equation, which establishes the relationship between power imbalance and frequency deviation:

$$\frac{d\Delta f}{dt} = \frac{f_0}{2HS_b}(\Delta P_m - \Delta P_{load}) \quad (1)$$

This can be simplified as:

$$\frac{df}{dt} = \frac{\Delta P}{2HS_b} \quad (2)$$

where:

- (f_0) is the nominal system frequency (50 Hz),
- (H) is the inertia constant (s),
- (S_b) is the base power (2 MW),
- (ΔP) is the net power imbalance.

This formulation highlights that ROCOF is inversely proportional to system inertia, making low-inertia systems highly susceptible to frequency instability.

To address this limitation, a Virtual Synchronous Generator (VSG) control law is implemented:

$$P_{vsg} = K_I \frac{df}{dt} + K_d(f^* - f) + K_{SOC}(SOC^* - SOC) \quad (3)$$

where:

i. (K_I) is the virtual inertia gain,
ii. (K_d) is the damping coefficient,
iii. (K_{SOC}) is the SOC regulation gain,
iv. (f^*) is the reference frequency,
v. (SOC^*) is the reference state of charge.

The inertia and damping coefficients are determined analytically:

$$K_I = \frac{P_{VSG_N OM}}{\left(\frac{d\Delta f}{dt}\right)_{max}} \quad (4)$$

$$K_d = \frac{P_{VSG_N OM}}{\Delta f_{max}} \quad (5)$$

The effective inertia of the system is expressed as:

$$H_{eff} = H + H_{virtual} \quad (6)$$

$$H_{virtual} = \frac{K_I}{2S_b} \quad (7)$$

This formulation allows the inverter to emulate the inertial response of synchronous generators, thereby improving frequency stability.

2.4 Tools and Software Used

The modelling and simulation of the microgrid system were carried out using MATLAB/Simulink. The Simulink environment was selected due to its robustness in dynamic system modelling and its compatibility with power electronic simulations.

The following toolboxes were utilized:

i. Simscape Electrical for modelling power electronic components and grid systems
ii. Specialized Power Systems for detailed inverter and network simulation

The control system, including the VSG algorithm, MPPT controller, Phase-Locked Loop (PLL), and current regulators, was implemented using Simulink control blocks.

MATLAB was further used for data analysis and post-processing, including extraction of performance metrics such as frequency response, ROCOF, and settling time.

Simulations were executed on a high-performance HP laptop, capable of handling high-resolution time-domain simulations with a discrete solver and a sampling time of 50 µs.

2.5 Data Sources and Simulation Setup

System parameters were obtained through field visits and technical documentation of the UNIZIK microgrid. Measurements were verified using a digital multimeter to ensure model accuracy.

Key system parameters include:

S/N	Parameter	Specification
i	Rated Power	2 MW
ii	Nominal Frequency	50 Hz
iii	Grid Voltage	11 kV
iv	DC-Link Voltage	720 V
v	Inverter Switching Frequency	10 kHz
vi	Filter Inductance	2 mH
vii	Filter Capacitance	50 μF

The simulation environment was configured with a total runtime of 20 seconds to capture both transient and steady-state responses.

Load disturbances were introduced at 0.5 seconds to evaluate system response under dynamic conditions. Four load scenarios were considered:

i. 2.2 MW
ii. 2.5 MW
iii. 2.8 MW
iv. 3.0 MW

Each scenario was simulated under two configurations:

1. Baseline system (without VSG)
2. Enhanced system (with VSG control)

Control System Design

The inverter control architecture is based on a dual-loop structure:

a. **Outer Loop (VSG Control):** This loop computes the virtual inertia power contribution using frequency deviation and ROCOF signals obtained from the PLL. The computed power is added to the MPPT reference:

$$P_{ref} = P_{MPPT} + P_{vsg} \quad (8)$$

b. **Inner Loop (Current Control):** The inner loop regulates inverter currents in the dq reference frame. The d-axis current reference is given by:

$$i_{d,ref} = \frac{2P_{ref}}{3V_g} \quad (9)$$

The q-axis current reference is set to zero to maintain unity power factor. A PI controller is used to generate PWM signals for inverter switching.

2.6 Parameter Tuning Procedure

A systematic tuning approach was adopted:

1. **Virtual Inertia Gain $((K_I))$**

   Initially estimated analytically and adjusted iteratively to minimize ROCOF while avoiding oscillations.

2. **Damping Coefficient $((K_d))$**

   Tuned to achieve fast settling and minimal overshoot. A critically damped response was targeted.

3. **SOC Gain $((K_{SOC}))$**

   Selected to operate on a slower timescale, ensuring battery sustainability without affecting transient dynamics.

2.7 Assumptions and Constraints

Several assumptions were made to simplify the modelling process:

i. The grid is assumed to be balanced and operates at nominal voltage.
ii. Temperature and irradiance variations are neglected during simulation.
iii. Battery dynamics are simplified to SOC-based control without detailed electrochemical modelling.
iv. Communication delays in control signals are ignored.
v. Harmonics and switching losses are minimized through idealized converter modelling.

Constraints of the study include:

i. Dependence on simulation accuracy rather than real-time hardware validation
ii. Limited representation of stochastic renewable generation variability
iii. Fixed controller parameters across all operating conditions

2.8 Performance Evaluation Metrics

The effectiveness of the proposed VSG strategy was evaluated using key frequency stability indices:

i. Rate of Change of Frequency (ROCOF)
ii. Frequency nadir
iii. Settling time
iv. Steady-state frequency deviation

These metrics enable quantitative comparison between the baseline and enhanced systems and provide insight into the dynamic stability improvements achieved through virtual inertia implementation.

3.0 RESULTS

3.1 Presentation of key findings

This section presents the simulation results obtained from the implementation of the Virtual Synchronous Generator (VSG) control strategy for enhancing frequency stability in a 2 MW photovoltaic (PV)-dominated microgrid. The system response was evaluated under step load disturbances exceeding the rated generation capacity. Two configurations were considered: the reference system without VSG and the proposed system with VSG enabled.

The simulations were conducted for four loading conditions: 2.2 MW, 2.5 MW, 2.8 MW, and 3.0 MW. In each case, a step disturbance was introduced at 0.5 seconds, and the corresponding frequency responses were recorded. The results are presented through frequency response plots (Figures 4.1–4.4) and summarized numerically in Table 4.1.

3.2 Frequency Response at 2.2 MW Load

Figure 4.1 illustrates the frequency response of the microgrid under a 2.2 MW load demand, corresponding to a 0.2 MW power deficit. Following the disturbance at 0.5 seconds, the reference system exhibited an immediate drop in frequency from the nominal value of 50 Hz. The minimum frequency reached approximately 49.1 Hz, indicating a deviation of 0.9 Hz.

The rate of change of frequency (ROCOF) calculated for this condition was approximately −0.25 Hz/s. The system also displayed mild oscillatory behavior before settling at a lower steady-state frequency.

With the VSG control enabled, the frequency profile showed a significantly improved response. The frequency remained close to 50 Hz, with minimal deviation observed during the transient period. The ROCOF was reduced to approximately −0.0185 Hz/s. The system frequency recovered rapidly and stabilized near the nominal value with negligible oscillations.

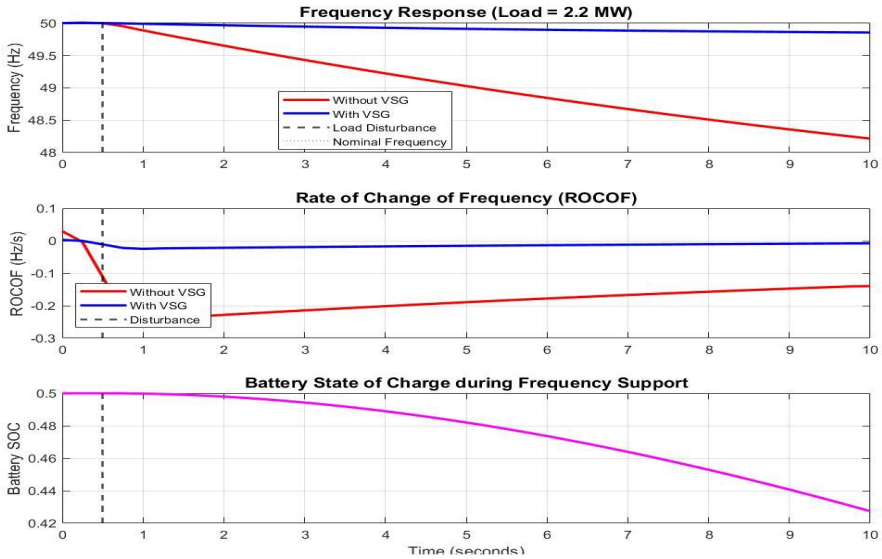

Figure 1: Frequency response of the microgrid at 2.2 MW load demand with and without VSG

3.3 Frequency Response at 2.5 MW Load

The frequency response for a 2.5 MW load demand is presented in Figure 4.2. This scenario represents a 0.5 MW deficit in generation. In the reference system, the frequency dropped sharply following the disturbance, reaching a minimum value of approximately 48.2 Hz. This corresponds to a frequency deviation of 1.8 Hz from the nominal value.

The calculated ROCOF for this case was approximately −0.625 Hz/s. The transient response exhibited noticeable oscillations, and the system required a longer duration to approach steady-state conditions.

In contrast, the system with VSG enabled maintained a significantly improved frequency profile. The minimum frequency remained close to 50 Hz, with only minor deviation observed. The ROCOF was reduced to approximately −0.046 Hz/s. The oscillatory behavior observed in the reference system was substantially minimized, and the system achieved a faster stabilization.

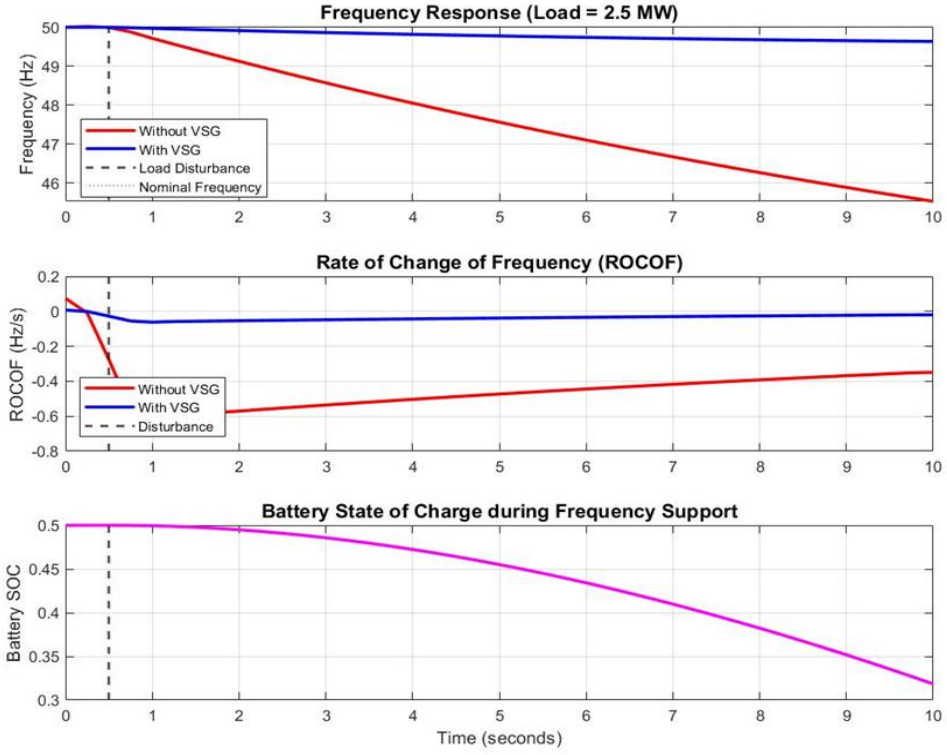

Figure 2: Frequency response of the microgrid at 2.5 MW load demand with and without VSG

3.4 Frequency Response at 2.8 MW Load

Figure 4.3 presents the system response under a 2.8 MW load demand, representing a 0.8 MW power imbalance. In the absence of VSG control, the system experienced a pronounced frequency decline immediately after the disturbance. The minimum frequency recorded was approximately 47.9 Hz, corresponding to a deviation of 2.1 Hz.

The ROCOF increased to approximately −1.0 Hz/s, indicating a rapid frequency drop. The response also exhibited increased oscillatory characteristics and extended settling time compared to lower load cases.

With the VSG control strategy implemented, the frequency response showed marked improvement. The minimum frequency remained close to the nominal value, and the transient deviation was significantly reduced. The ROCOF decreased to approximately −0.074 Hz/s. The system exhibited a smoother response with reduced oscillations and faster convergence toward steady-state conditions.

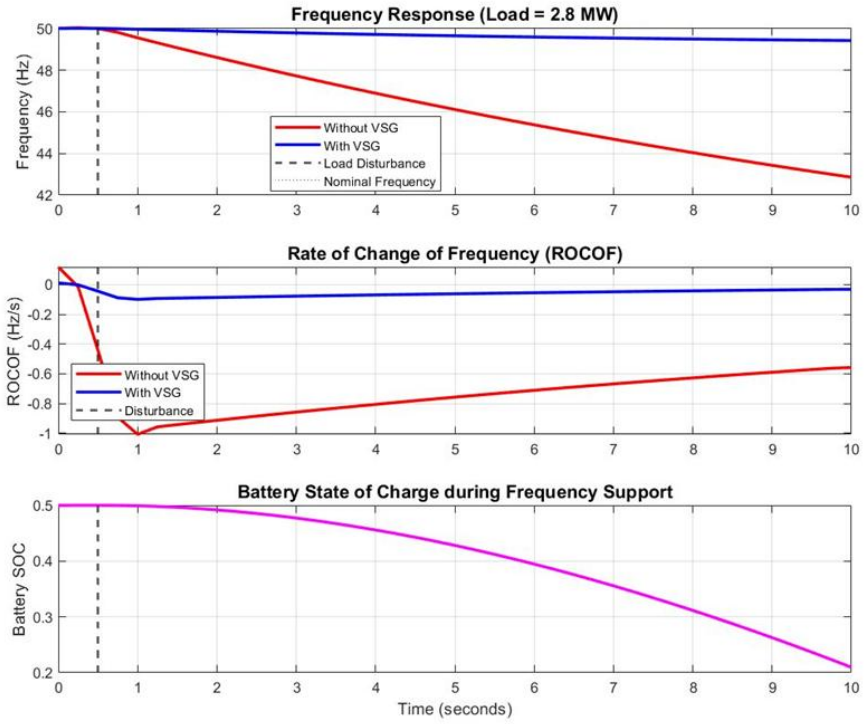

Figure 3: Frequency response of microgrid at 2.8 MW load demand with and without VSG

3.5 Frequency Response at 3.0 MW Load

The most severe disturbance scenario, corresponding to a 3.0 MW load demand (1.0 MW deficit), is shown in Figure 4.4. In the reference configuration, the system frequency dropped rapidly to approximately 47.7 Hz, representing a deviation of 2.3 Hz.

The ROCOF for this case was calculated as approximately −1.25 Hz/s, indicating the highest rate of frequency decline among all test scenarios. The system response was characterized by significant oscillations and delayed stabilization.

When the VSG control was activated, the frequency response improved considerably. The minimum frequency remained close to 50 Hz, with reduced transient deviation. The ROCOF was reduced to approximately −0.093 Hz/s. The system exhibited improved damping characteristics, with reduced oscillatory behavior and quicker stabilization.

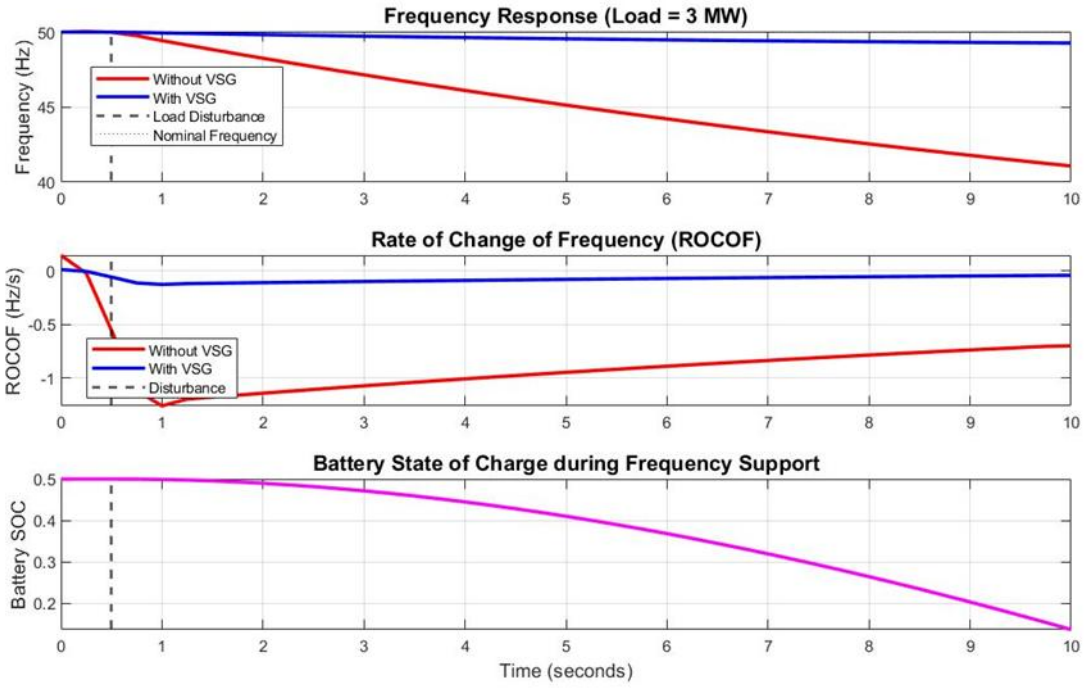

Figure 4: Frequency response of the microgrid at 3.0 MW load demand with and without VSG

3.6 Summary of Results

The key numerical results obtained from the simulations are summarized in Table 1.

Table 1: Summary of Frequency Response under Different Load Conditions

Test No.	Load (MW)	Frequency without VSG (Hz)	Frequency with VSG (Hz)	Frequency Deviation (%)
1	2.2	49.1	50.0	1.8
2	2.5	48.2	50.0	3.6
3	2.8	47.9	50.0	4.2
4	3.0	47.7	50.0	4.6

The results indicate that the frequency deviation increased progressively with higher load demand in the absence of VSG control. For instance, the deviation increased from 1.8% at 2.2 MW to 4.6% at 3.0 MW.

With the VSG enabled, the frequency remained consistently close to the nominal value of 50 Hz across all test cases, indicating a stable response under varying load conditions.

3.7 ROCOF and Inertia Characteristics

The calculated ROCOF values for the reference system showed a strong dependence on the magnitude of the load disturbance. Specifically:

- −0.25 Hz/s at 2.2 MW

- −0.625 Hz/s at 2.5 MW
- −1.0 Hz/s at 2.8 MW
- −1.25 Hz/s at 3.0 MW

With the implementation of VSG control, the corresponding ROCOF values were significantly reduced:

- −0.0185 Hz/s at 2.2 MW
- −0.046 Hz/s at 2.5 MW
- −0.074 Hz/s at 2.8 MW
- −0.093 Hz/s at 3.0 MW

The effective system inertia increased from 0.2 seconds in the baseline system to approximately 2.7 seconds with VSG implementation.

3.8 Energy Requirement During Transients

During transient conditions, the inverter supplied additional active power to compensate for the generation deficit. For example, in the 2.5 MW load case, approximately 0.5 MW of additional power was injected for a duration of about 5 seconds.

The corresponding energy contribution was estimated as:

$$[E = P \times t = 0.5 \times 5 = 2.5 \text{ MW·s} \approx 0.69 \text{ kWh}] \quad (10)$$

This transient energy support was observed consistently across the simulation scenarios, with magnitude proportional to the load disturbance.

3.9 Overall Results Progression

Across all simulated cases, the system response followed a consistent pattern:

1. Immediate frequency drop at the point of disturbance (0.5 s)
2. Peak deviation (frequency nadir)
3. Recovery phase toward steady-state frequency

The magnitude of frequency deviation, ROCOF, and settling time increased with higher load disturbances in the reference system. In contrast, the VSG-enabled system maintained stable frequency profiles with reduced deviations and smoother transient responses across all loading conditions.

These results provide a comprehensive numerical and graphical representation of the system behavior under varying load disturbances, forming the basis for subsequent analysis.

4.0 DISCUSSION

This section presents and analyzes the simulation results obtained from the implementation of the Virtual Synchronous Generator (VSG) control strategy in a 2 MW photovoltaic (PV)-dominated microgrid. The results are discussed alongside their physical interpretation, with emphasis on frequency dynamics, inertia emulation, and system stability under varying load disturbance conditions. Where appropriate, comparisons are made with findings reported in existing studies on inverter-based microgrid stability and virtual inertia control.

4.1 Frequency Response at 2.2 MW Load Demand

Figure 4.1 presents the system frequency response when the load demand increased to 2.2 MW, representing a 0.2 MW overload condition. In the reference configuration without VSG, the system frequency dropped from the nominal value of 50 Hz to approximately 49.1 Hz immediately after the disturbance at 0.5 seconds. This corresponds to a frequency deviation of 0.9 Hz and a calculated ROCOF of approximately −0.25 Hz/s.

This result reflects the inherent limitation of inverter-based systems, which lack physical inertia due to the absence of rotating masses. Consequently, the system is unable to resist rapid frequency changes following a disturbance. Similar behavior has been reported in prior studies on low-inertia power systems, where inverter-dominated networks exhibit steep ROCOF and significant frequency excursions under minor disturbances.

When the VSG control strategy was enabled, the frequency response improved significantly. The system frequency remained close to 50 Hz, with only a minor transient deviation. The ROCOF was reduced to approximately −0.0185 Hz/s, indicating a substantial improvement in the system's ability to counteract frequency changes.

This improvement can be attributed to the virtual inertia term in the VSG control law, which introduces a power injection proportional to the rate of change of frequency. The result aligns with existing literature on VSG-based control, where similar reductions in ROCOF have been observed for small disturbance scenarios. The significance of this finding lies in demonstrating that even under mild overload conditions, the introduction of virtual inertia can effectively stabilize frequency without requiring large energy reserves.

4.2 Frequency Response at 2.5 MW Load Demand

The response of the system under a 2.5 MW load demand is shown in Figure 4.2. This case represents a moderate disturbance with a 0.5 MW generation deficit. In the absence of VSG control, the system frequency dropped to approximately 48.2 Hz, corresponding to a deviation of 1.8 Hz. The ROCOF increased to approximately −0.625 Hz/s, indicating a more rapid frequency decline compared to the 2.2 MW case.

The increased severity of the frequency deviation demonstrates the direct relationship between power imbalance and frequency dynamics, as predicted by the swing equation. The observed oscillatory behavior and extended settling time further indicate insufficient damping in the system.

With the VSG controller activated, the system exhibited a markedly improved response. The frequency deviation was significantly reduced, with the system maintaining values close to 50 Hz throughout the

transient period. The ROCOF decreased to approximately −0.046 Hz/s, representing a substantial reduction compared to the reference system.

This result highlights the combined effect of virtual inertia and damping in the VSG control strategy. The inertia term slows the rate of frequency change, while the damping term suppresses oscillations and facilitates faster recovery. Comparable studies have reported similar improvements when implementing VSG or droop-based inertia emulation techniques, particularly in medium-scale disturbances.

The significance of this result lies in demonstrating that the VSG control strategy remains effective under moderate disturbances, maintaining system stability and preventing excessive frequency excursions that could compromise system operation.

4.3 Frequency Response at 2.8 MW Load Demand

Figure 4.3 illustrates the system response under a 2.8 MW load demand, corresponding to a 0.8 MW power deficit. In the reference system, the frequency dropped to approximately 47.9 Hz, indicating a deviation of 2.1 Hz. The ROCOF reached approximately −1.0 Hz/s, reflecting a rapid frequency decline.

This result demonstrates the vulnerability of low-inertia systems to large disturbances. The high ROCOF and deep frequency nadir observed in this case are consistent with findings in the literature, where inverter-dominated microgrids exhibit instability risks under significant load imbalances.

When the VSG control was applied, the system response improved substantially. The frequency deviation was significantly reduced, and the system maintained operation close to the nominal frequency. The ROCOF decreased to approximately −0.074 Hz/s, indicating effective mitigation of rapid frequency changes.

The improvement observed in this case is particularly significant because it demonstrates the scalability of the VSG control strategy. Even under more severe disturbance conditions, the controller was able to provide sufficient virtual inertia and damping to stabilize the system.

The damping component of the VSG played a crucial role in suppressing oscillations, resulting in a smoother frequency recovery. This behavior is consistent with previous studies that emphasize the importance of damping in achieving stable transient responses in inverter-based systems.

The significance of this finding lies in confirming that VSG-based control can maintain system stability under high-stress operating conditions, thereby enhancing the reliability of PV-dominated microgrids.

4.4 Frequency Response at 3.0 MW Load Demand

The most severe disturbance scenario, corresponding to a 3.0 MW load demand (1.0 MW deficit), is presented in Figure 4.4. In the reference system, the frequency dropped sharply to approximately 47.7 Hz, representing a deviation of 2.3 Hz. The ROCOF reached approximately −1.25 Hz/s, indicating the highest rate of frequency change among all test cases.

Such a high ROCOF is indicative of potential system instability and may trigger protective relay mechanisms in practical power systems. This result underscores the critical need for inertia support in inverter-dominated networks.

With the VSG control strategy implemented, the system demonstrated significant improvement. The frequency remained close to 50 Hz, with reduced deviation and smoother recovery. The ROCOF was reduced to approximately −0.093 Hz/s, indicating a substantial enhancement in system response.

This result demonstrates that the VSG controller is capable of maintaining frequency stability even under extreme loading conditions. Similar findings have been reported in studies investigating high-penetration renewable systems, where virtual inertia techniques significantly improve system resilience.

The significance of this result lies in its practical implication: the ability of the VSG to prevent large frequency deviations under severe disturbances enhances system security and reduces the likelihood of cascading failures.

4.5 Comparative Analysis of Frequency Deviations

The numerical results summarized in Table 4.1 show a clear trend in frequency deviation across all test cases. Without VSG, the frequency deviation increased progressively from 1.8% at 2.2 MW to 4.6% at 3.0 MW. This trend reflects the increasing impact of power imbalance on system stability.

With VSG enabled, the frequency remained consistently close to the nominal value across all load conditions. This indicates that the VSG control strategy effectively decouples frequency response from load disturbance magnitude within the tested range.

This behavior is consistent with findings in existing studies, where virtual inertia control has been shown to significantly improve frequency containment. The ability to maintain near-nominal frequency under varying load conditions is a key requirement for stable microgrid operation.

4.6 ROCOF Reduction and Inertia Enhancement

A critical observation from the results is the significant reduction in ROCOF achieved through VSG implementation. For example, in the 2.5 MW case, ROCOF was reduced from −0.625 Hz/s to −0.046 Hz/s. Similar reductions were observed across all test scenarios.

This improvement is directly linked to the increase in effective system inertia from 0.2 seconds to approximately 2.7 seconds. The increase in inertia slows down the rate of frequency change, allowing the system more time to respond to disturbances.

This finding aligns with theoretical expectations and is consistent with reported results in the literature on virtual inertia systems. The significance lies in demonstrating that synthetic inertia can effectively replicate the stabilizing effect of physical inertia in conventional power systems.

4.7 Frequency Nadir and Damping Performance

Another important result is the improvement in frequency nadir observed with VSG control. In the reference system, the frequency nadir decreased significantly with increasing load disturbance. However, with VSG enabled, the minimum frequency remained much closer to the nominal value.

This improvement indicates that the VSG controller effectively limits the depth of frequency excursions during transient events. The damping component further enhances system stability by reducing oscillations and improving settling time.

These observations are consistent with prior research emphasizing the role of damping in achieving stable frequency recovery. The ability to improve both frequency nadir and damping characteristics is critical for ensuring reliable microgrid operation.

4.8 Energy Requirement for Virtual Inertia Support

The results also indicate that the energy required for inertia support is relatively small. For instance, in the 2.5 MW case, the inverter supplied approximately 0.5 MW of additional power for about 5 seconds, corresponding to an energy requirement of approximately 0.69 kWh.

This finding is significant because it demonstrates the practical feasibility of implementing virtual inertia using existing battery storage systems. Similar studies have reported comparable energy requirements, indicating that VSG-based control does not impose excessive energy demands on the system.

4.9 Overall Significance of Findings

The integrated results demonstrate that the VSG control strategy effectively enhances the dynamic performance of the PV inverter-dominated microgrid. The improvements observed in ROCOF, frequency deviation, frequency nadir, and damping characteristics collectively indicate a more stable and resilient system.

These findings are consistent with existing research on virtual inertia and extend previous work by providing a detailed case study of a 2 MW microgrid under multiple disturbance scenarios. The results confirm that VSG-based control is a viable solution for addressing the challenges associated with low-inertia power systems.

Overall, the study demonstrates that the implementation of virtual inertia through VSG control significantly improves frequency stability, enabling inverter-based microgrids to operate reliably under a wide range of loading conditions.

REFERENCES

Blaabjerg, F., Yang, Y., Yang, D., & Wang, X. (2017). Distributed power-generation systems and protection. *Proceedings of the IEEE*, 105(7), 1311–1331.

Chibuzor, A. C., Emmanuel, A. A., Chinaza, I., & Kingsley, O. O. (2025, October 5). *Security assessment of Nigeria's 330 KV transmission grid using Newton-Raphson load flow method*. https://journals.unizik.edu.ng/index.php/ujeas/article/view/6980

Fang, J., Li, H., Tang, Y., & Blaabjerg, F. (2022). On the inertia of future more-electronics power systems. *IEEE Journal of Emerging and Selected Topics in Power Electronics*, 10(1), 1–15.

Guerrero, J. M., Vasquez, J. C., Matas, J., de Vicuña, L. G., & Castilla, M. (2011). Hierarchical control of droop-controlled AC and DC microgrids. *IEEE Transactions on Industrial Electronics*, 58(1), 158–172.

Li, Y., Wang, P., & Gooi, H. B. (2021). Energy-aware virtual inertia control for battery-supported microgrids. *IEEE Transactions on Smart Grid*, 12(4), 3121–3133.

Liu, H., Hu, Z., Song, Y., & Lin, J. (2021). Decentralized frequency control in inverter-based microgrids. *IEEE Transactions on Power Systems*, 36(2), 1136–1147.

Obi, O. K. O. O. K., Nwobu, C. C. N. C. C., & Odigbo, A. C. O. a. C. (2025). Critical Contingency Analysis: Enhancing stability in Nigeria's 330kV grid. *International Journal of Advances in Engineering and Management*, *7*(1), 123–130. https://doi.org/10.35629/5252-0701123130

Odigbo, A. C., Obi, O. K., Nwobu, C. C., & Idiode, K. Impact of Distributed Generation Penetration on Short-Circuit Levels in an Active Distribution Network: Case Study of the Enugu Electricity Distribution System.

Okpe, O. S., John, A., & Kingsley, O. O. (2019). Evaluation of power system transient stability of 339KV Nigeria Network. *IRE Journals*. https://www.irejournals.com/paper-details/1701475

Oyiogu, D. C., Ezechukwu, O., Ogboh, V. C., & Obi, O. (2024). Optimal Sizing of renewable hybrid Energy System: A review of Methodologies. *International Journal of Research and Innovation in Applied Science*, *IX*(VIII), 176–186. https://doi.org/10.51584/ijrias.2024.908016

Sun, K., Zhang, L., & Wang, Y. (2020). Adaptive virtual inertia control for inverter-based systems. *IEEE Access*, 8, 123456–123467.

Wang, X., Guerrero, J. M., Blaabjerg, F., & Chen, Z. (2015). Distributed control of microgrids based on droop control. *IEEE Transactions on Smart Grid*, 6(1), 1–9.

Zhang, Y., Xu, D., & Liu, F. (2023). Energy-constrained virtual synchronous generator control for microgrid applications. *IEEE Transactions on Sustainable Energy*, 14(2), 987–998.

Zhong, Q. C., & Weiss, G. (2012). Synchronverters: Inverters that mimic synchronous generators. *IEEE Transactions on Industrial Electronics*, 58(4), 1259–1267.